

# Fuel flexibility of a 100kW<sub>e</sub> micro gas turbine: Combustion performance using natural gas and non-conventional syngas

J. Bompas<sup>1</sup>, W. De Paepe<sup>1</sup>

<sup>1</sup> University of Mons (UMONS), Faculté Polytechnique, Rue de l'Épargne, 7000 Mons, Belgium

## ABSTRACT

Worldwide electricity consumption is still increasing while there is the clear ambition to reduce greenhouse gas emissions. To ensure sufficient sustainable electricity resources for our society, an energy source diversification is necessary. Indeed, next to high potential but intermittent renewable energies like wind and solar, traditional thermal power production using renewable resources like syngas and biogas are good candidates to achieve these energy mix goals. However, given their specific properties, i.e., having a lower energy content, better characterization of these non-conventional energy sources in their combustion behavior is needed.

In this work, we compare the combustion behavior of syngas with natural gas in the complex geometry of a typical mGT combustor, the Turbec T100. A first approach includes the development of a turbulent combustion model that allows to validate the temperature fields and species concentration gradients for natural gas, reference case, in known conditions. In a second step, we aim to get some first insight on the impact of using syngas through injection in the main flame. The results show that temperature and velocity fields for both natural and syngas combustion can be correctly predicted. Moreover, it was possible to get an accurate prediction on intermediate species and NO<sub>x</sub>, CO, CO<sub>2</sub> and H<sub>2</sub>O in the flue gases. These obtained results will serve as benchmark for future characterization for a specific range of diluted inlet conditions of various syngases and biogases, which will allow to fully exploit its potential in small-scale cogeneration application.

**Keywords:** CFD, micro gas turbine, renewable energy, syngas, emission

## NOMENCLATURE

### Abbreviations

DES	Decentralized Energy System
CHP	Combined Heat and Power
MGT	Micro Gas Turbine
RANS	Reynolds Averaged Navier-Stokes
EDC	Eddy Dissipation Concept

### Symbols

$\dot{m}$	mass flow rate (g/s)
$Y_i$	mass fraction of species i (-)
T	Temperature (K)

## 1. INTRODUCTION

In the last years, the investments in renewable energy are massively strengthened. Electricity consumption (increasing), fossil fuels availability (decreasing), pollutant emission policy (reducing) are clearly contributing to this interest [1]. Next to wind and solar energies, renewable resources like syngas and biogas offer great opportunities to partially replace natural gas in the energy mix and by doing so, leading to a significant CO<sub>2</sub> emissions reduction.

Considering the current trend of shifting from centralized electricity production to more decentralized system (DES), micro gas turbines (MGT) represent themselves as relevant conversion system for the realization of a smart energy grid. The versatility of using a wide range of fuels and the flexibility of MGT in the cycle of an efficient Combined Heat and Power (CHP) system is leading to attractive research in decentralized domestic energy production.

However, the diversity of fuels and the wide variation of their properties requires to better characterize non-conventional fuel combustion behavior. Despite the availability of past research [2,3,4,5,6], several key aspects towards the stable and complete combustion of syngas in mGT combustors, i.e., flame stability, emission control and pilot/main fuel control, remain unclear and require further research. The aim of the paper is thus to provide a base for the application of syngas in natural gas setup MGTs and the improvement in combustion conditions of small-scale cogeneration application.

## 2. TURBEC T100 COMBUSTION CHAMBER

### 2.1 Geometry

The Turbec T100 is a typical micro gas turbine system for CHP applications. The nominal electrical power output is 100 kW<sub>e</sub> and the corresponding thermal power output is about 165 kW<sub>th</sub>, with an electrical efficiency of about 30% and an 80% overall efficiency [7]. The T100 operates according to the recuperated Brayton cycle and exploits a variable speed centrifugal compressor and turbine system. By means of a mixed counter/cross-flow recuperator, compressed air is preheated by the flue gases before entering the combustion chamber, leading to superior electric performance.

The combustion chamber, considered in this study, is a reverse flow tubular combustor [8]. The fuel is injected in two different lines (see Fig. 1): the pilot line using 6 nozzles (diffusion flame) and the main line composed by a toroidal chamber injecting by means of 15 nozzles (premixed flame).

The pre-heated air from the recuperator, entering the combustion chamber in countercurrent, is divided over



**Figure 1.** Schematic cross section of T100 combustor, highlighting the counter-flow air inlet on the outside of the chamber, as well as the pilot (1) and main (2) flame injectors, as well as the dilution holes.

**Table 1** Flow distribution in Turbec T100

	nb	Dimension	Distribution
Dilution holes	9	D = 20 (mm)	60.1 %
Cylinder swirler 1	12	D = 3.5 (mm)	2.5 %
Annular swirler 2	1	D <sub>e</sub> = 34 (mm) D <sub>i</sub> = 28 (mm)	24,9 %
Cylinder swirler 2'	30	D = 5 (mm)	12.5 %

different sections: The swirlers 1 (12 jet holes) provide the air to the pilot flame (approximately 2.5%) while swirlers 2 (15 radial vanes) and 2' (30 jet holes) supply the air for the main flame (respectively 24.9% and 12.5%)<sup>1</sup>. Additionally, the remaining part of the incoming air is passing through nine dilution holes to reduce the temperature of the flue gases to limit the turbine inlet temperature to 950°C. Finally, Table 1 summarizes the air distribution as well as the specific dimensions of each part.

### 2.2 Mesh analysis

The generated mesh included the entire fluid domain of the combustion chamber without simplifications: e.g., as opposed to many researchers, in this study the countercurrent inlet air section has been included as well (Fig. 2). Due to the complex geometry of the Turbec T100, a fully 3-dimensional hexahedral mesh generation was adopted. A specific refinement has been realized on the complex shapes of the swirlers and the primary combustion zone. A finer discretization has been set for the small elements of pilot and main fuel nozzles (see Fig. 2).

A preliminary mesh sensitivity study has been conducted to determine the appropriate mesh size. The study indicated that a mesh consisting in 4.2 million cells is sufficient refined to provide accurate and mesh

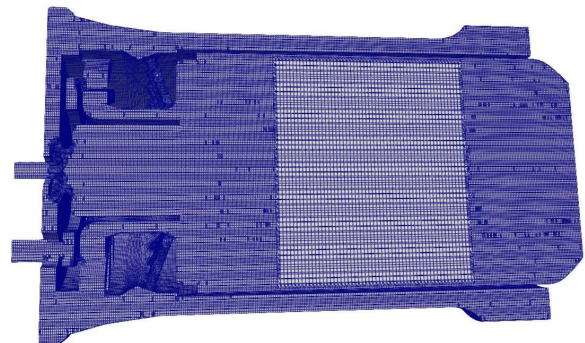


**Figure 2.** Hexahedral grid cross-section of T100

<sup>1</sup> Air distribution obtained with simulation results (see results section) and are in agreement with values obtained by [8]

independent results. Moreover, similar mesh sizes have been used by other researchers, performing similar RANS simulations on the same combustor [7].

### 2.3 Numerical setup

A preliminary study was conducted to determine and select the appropriate models to the numerical simulations. The turbulence model is based on Reynolds Averaged Navier-Stokes (RANS) approach, more specifically the robust  $k-\epsilon$  turbulence model.

The Eddy Dissipation Concept [9] was selected and implemented as combustion model. EDC is admitted as the most reliable model given the presence of both diffusive (pilot) and premixed flame (main). Since the chemical reaction rate depends essentially on the time needed to mix the reagents in molecular fine structure, the reacting part is modeled as a perfectly stirred reactor.

To correctly capture the intermediary reactants and improve the accuracy on the unburned species in the flue gases, the GRI-3.0 mechanism [10] thermophysical model is used. It modeled the kinetics of 53 species in 325 reactions, examining the sensitivity of each reaction to better predict the occurrence of the different species in the combustion. This detailed mechanism is particularly interesting in the detection of  $\text{NO}_x$  and CO for the analysis of the combustion.

### 2.4 Boundary conditions

To characterize the flow in the combustion chamber, a first numerical simulation has been carried out (See Table 2, Case a), using pure methane injection in the T100 at full load conditions of 100 kW<sub>e</sub>. The air distribution ensures a sufficient excess air throughout the combustion. The air mass flow rate was determined based on previously validated thermodynamic cycle analysis [11], whereas the main and pilot fuel injection was set similar to the settings used by De Santis et al. [2]. The second simulation (see Table 2, Case b) is performed using again pure methane as fuel and considering a 33%

**Table 2** Boundary conditions CH<sub>4</sub> a) 100 kW<sub>e</sub> b) 133 kW<sub>e</sub>

		Pilot fuel	Main fuel	Air
$\dot{m}$ (g/s)	a)	0.8	5.7	690
	b)	0.8	7.2	750
$Y_i$ (—)	a), b)	$Y_{\text{CH}_4}: 100\%$		$Y_{\text{O}_2}: 23\%$ $Y_{\text{N}_2}: 77\%$
T(K)		288		865

**Table 3** Mass fraction  $Y_i$  (%) composition of Syngas

$Y_{\text{CO}}$	$Y_{\text{CO}_2}$	$Y_{\text{H}_2\text{O}}$	$Y_{\text{H}_2}$	$Y_{\text{CH}_4}$	$Y_{\text{N}_2}$
55.1	31.8	7.8	3.8	1.4	0.16

higher air and fuel mass flow rate compared to nominal conditions (case a). This corresponds to a theoretical 133 kW<sub>e</sub> electric power output. This simulation allows to analyze the combustor flexibility under higher flow rates, while keeping the excess air range suitable with a stabilized flame in both primary and secondary combustion chamber.

In the third case, the main fuel inlet is fed with a fuel obtained by a gasification process (Syngas) without changing the geometry of the combustor, historically designed for natural gas. To ignite the combustion and ensure a stabilized diffusion flame in the primary chamber, pure methane is still injected to supply the pilot flame using identical conditions as in the methane cases, i.e., flow rate and temperature. The specific composition of the Syngas is presented in Table 3. Furthermore, the same boundary conditions as for the natural gas cases have been set (e.g., air mass flow rate and temperature, see Table 4), except for the fuel mass flow rate that must be, obviously, increased to maintain the input thermal power constant, considering the corresponding LHV of Syngas being only 10.8 MJ/kg (50.1 MJ/kg for pure CH<sub>4</sub>).

**Table 4** Boundary condition SYNGAS c) 100 kW<sub>e</sub>

	$\dot{m}$ (g/s)	Specie	T(K)
Pilot fuel inlet	0.8	CH <sub>4</sub>	288
Main fuel inlet	27.5	SYNGAS	288
Air inlet	750	$Y_{\text{O}_2}: 23\%$ $Y_{\text{N}_2}: 77\%$	865

## 3. RESULTS

Within this preliminary study, we focused first on the main quantities of interest, being flow field, temperature field and global flue gas composition, aiming at validating the reference case (case a), as well as studying the impact of altering the thermal energy input (case b) and the type of fuel (case c).

Combustion under nominal operating conditions using pure methane (case a), leads to typical flow and temperature fields as those found in literature (Fig. 3 and 4, [7]). Concerning the flow field, the different recirculation zones, resulting from the swirl flow are well captured. Moreover, the temperature peaks, related to

**Table 4** Exhaust gas composition

	$Y_i(\%)$		
	a) CH <sub>4</sub>	b) CH <sub>4</sub>	c) SYNGAS
O <sub>2</sub>	18.2	17.5	19.9
N <sub>2</sub>	75.7	75.8	74.7
CO <sub>2</sub>	3.3	3.8	3.8
H <sub>2</sub> O	2.6	2.9	1.5
CO	2 ppmv	4 ppmv	3 ppmv
NO <sub>x</sub>	11 ppmv	14 ppmv	9 ppmv
T <sub>out</sub> [K]	1333	1386	1165

the pilot and main flame are also well capture when compared to DeSantis et al. [7].

Increasing the main fuel flow rate in case b and c (respectively for natural gas and syngas) and the air flow rate naturally increases the velocity field level in the premixed secondary swirlers (see Fig. 3). The morphology and the position of vortexes are not modified and the dynamic behavior in the main fuel line is not significantly affected. On the contrary, the temperature distribution is clearly influenced by the fuel and air distribution in terms of flame configuration.

In case b (see Fig. 4), the higher power input (+33%) and the reduction of air dilution explain the higher temperature levels compared to the standard configuration a). The lower temperature levels of the syngas case (c) are due to the dilution of the gas mixture for an equal power input [12].

Finally, the exhaust gas composition of the 3 different cases, presented in Table 4, correspond to equilibrium calculations for the main species, i.e., O<sub>2</sub>, N<sub>2</sub>, CO<sub>2</sub> and H<sub>2</sub>O. The CO and NO<sub>x</sub> emissions strongly depend

on the excess air coefficient and combustion flame temperature [13] but are within the range of the values reported by the manufacturer [14]. The use of Syngas results in lower temperature at the outlet, as well as within the chamber itself, with a substantial reduction of NO<sub>x</sub> emissions as results. The lower outlet temperature can be explained by the diluting effect due to the important syngas mass flow rate, while the lower chamber temperature levels are a result of the slower reaction rate of the syngas. Similar syngas and natural gas carbon monoxide levels indicate that the combustion efficiency is not significantly affected by the use of syngas (see Table 4).

#### 4. CONCLUSION

The paper presented preliminary numerical simulations performed on the Turbec T100 combustor fed by natural gas and a synthesis gas, aiming at studying its impact on emissions and combustion stability.

Besides energy source diversification environmental aspects, using syngas is promising on combustion process by lowering temperature in the combustion zone and consequently reducing NO<sub>x</sub> emissions. The CFD analysis has demonstrated the capability of numerical models in solving turbulent combustion of synthesis gases with different complex mixture composition.

However, further numerical simulations must be carried out to evaluate the performance of the combustion chamber when also the pilot flame is fed with syngas, towards emissions and flame stability. Moreover, the impact of switching to untreated syngas (having an important steam fraction), will be studied as well.

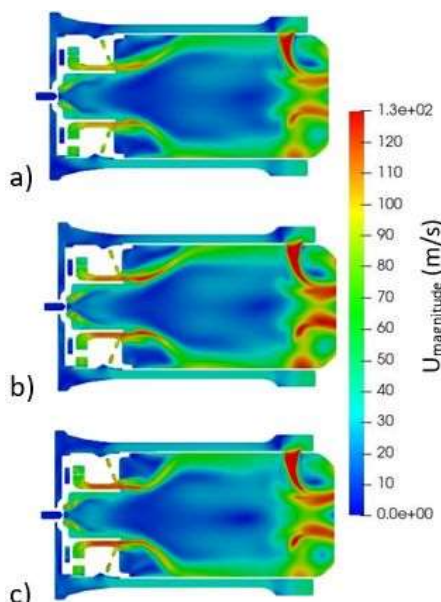


**Figure 3.** Velocity field of: a) Natural gas 100kW<sub>e</sub>  
b) Natural gas 133 kW<sub>e</sub> c) Syngas 100kW<sub>e</sub>

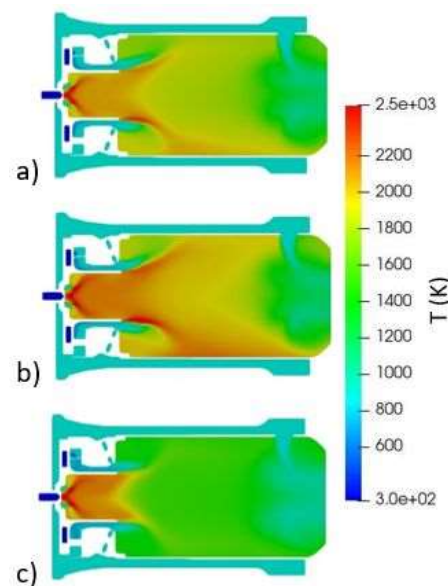


**Figure 4.** Temperature field of: a) Natural gas 100 kW<sub>e</sub>  
b) Natural gas 133 kW<sub>e</sub> c) Syngas 100 kW<sub>e</sub>

## ACKNOWLEDGEMENT

The authors would like to acknowledge the financial support received from the European Regional Development Fund (ERDF project).

Computational resources have been provided by the Consortium des Équipements de Calcul Intensif (CÉCI), funded by the Fonds de la Recherche Scientifique de Belgique (F.R.S.-FNRS) under Grant No. 2.5020.11 and by the Walloon Region

## REFERENCE

- [1] International Energy Agency Bioenergy, Contributions of sustainable biomass and bioenergy in industry transitions towards a circular economy. Summary and conclusions from the IEA Bioenergy eWorkshop; 2020. Available from: <https://www.ieabioenergy.com/>
- [2] Chiaramonti D, Rizzo AM, Spadi A, Prussi M, Riccio G, Martelli F. Exhaust emissions from liquid fuel micro gas turbine fed with diesel oil, biodiesel and vegetable oil. *Applied Energy*.
- [3] Cameretti MC, Tuccillo R. Combustion analysis in a micro-gas turbine supplied with bio-fuels. *ASME Conference Proceedings*2014.
- [4] Mirzamohammad N, Razbani O, Assadi M. Review of theoretical and experimental studies implemented on (CHP) Micro turbine using natural gas and biogas fuels. *Third International Conference on Applied Energy*2011.
- [5] Camporeale SM, Fortunato B, Torresi M, Turi F, Pantaleo AM, Pellerano A. Part load performance and operating strategies of a natural gas-biomass dual fuelled microturbine for CHP generation. *ASME Conference Proceedings*2014.
- [6] Nikpey H, Assadi M, Breuhaus P. Experimental investigation of the performance of a micro gas turbine fueled with mixtures of natural gas and biogas. *ASME Conference Proceedings*2013.
- [7] Andrea De Santis et al. CFD analysis of exhaust gas recirculation in a micro gas turbine combustor for CO<sub>2</sub> capture. *Fuel*. 2016;173:146-154. Available from: <https://doi.org/10.1016/j.fuel.2016.01.063>
- [8] Raffaella Calabria et al. Numerical of a micro gas turbine fed by liquid fuels: potentialities and critical issues. *Energy Procedia [Internet]*. 2015;81:1131-42. Available from: <http://dx.doi.org/10.1016/j.egypro.2015.12.138>
- [9] E. Ghasemi et al. RANS simulation of methane-air burner using local extinction approach within eddy dispersion concept by OpenFOAM. *International Communications in Heat and Mass Transfer*. 2014;54:96-102. Available from:

<https://doi.org/10.1016/j.icheatmasstransfer.2014.03.006>

- [10] G.P. Smith, D.M. Golden, M. Frenklach, N.W.Moriarty, B. Eiteneer, M. Goldenberg, C.T. Bowman, R. Hanson, S. Song, W.C. Gardiner, Jr., V.Lissianski, Z. Qin. Available at: [http://www.me.berkeley.edu/gri\\_mech/](http://www.me.berkeley.edu/gri_mech/)
- [11] De Paepe W, Montero Carrero M, Giorgetti S, Parente A, Bram S, Contino F. Exhaust Gas Recirculation on Humidified Flexible Micro Gas Turbines for Carbon Capture Applications. *ASME Conference Proceedings: ASME Turbo Expo 2016*. Paper Number GT2016-57265, V003T06A011.
- [12] M. Cadorin et al. Analysis of a micro gas turbine fed by natural gas and synthesis gas: Test bench and combustor CFD analysis. In: *Proceedings of the ASME Turbo Expo*. American Society of Mechanical Engineers (ASME); 2011.
- [13] Xiaoyu Chen et al. Numerical Analysis of the Combustion in Micro Gas Turbine with Methane/Biogas Fuels. *Arabian Journal for Science and Engineering*. Available from: <https://doi.org/10.1007/s13369-021-05731-3>
- [14] Turbec T100 microturbine system Natural Gas: Technical description v3. 2009.